



Sandwich-structured CeO₂@ZSM-5 hybrid composites for catalytic oxidation of 1, 2-dichloroethane: An integrated solution to coking and chlorine poisoning deactivation

Qiguang Dai*, Wei Wang, Xingyi Wang*, Guanzhong Lu

Key Lab for Advanced Materials, Research Institute of Industrial Catalysis, School of Chemistry & Molecular Engineering, East China University of Science and Technology, Shanghai, 200237, PR China



ARTICLE INFO

Article history:

Received 21 July 2016

Received in revised form 3 October 2016

Accepted 6 October 2016

Available online 6 October 2016

Keywords:

CVOCs

Deactivation

CeO₂

ZSM-5

Coking

ABSTRACT

Sandwich-structured CeO₂@HZSM-5 core-shell hybrid composites were designed and prepared by an *in situ* two-step hydrothermal growth method under dynamic condition, and SEM indicated that CeO₂ nanosheets were completely encapsulated by HZSM-5 particles which formed continuous and dense zeolite membranes (exposed HZSM-5). The catalytic total oxidation of 1, 2-dichloroethane (DCE) over CeO₂@HZSM-5 was investigated, compared with CeO₂/HZSM-5 (CeO₂ dispersed on HZSM-5) and CeO₂ + HZSM-5 (CeO₂ mixed with HZSM-5) reference catalysts. Although the latter two showed a better catalytic activity due to the synergies of ceria and HZSM-5 zeolite, the formation of poly-chlorinated hydrocarbons (PCHs) by-products over CeO₂@HZSM-5 was significantly inhibited since CeO₂ with high activity for Deacon reaction was not directly exposed to DCE or HCl molecules. Moreover, CeO₂@HZSM-5 also exhibited a better resistance to the coking and chlorine poisoning, because the formed non-activated coke species or polyaromatic species could be easier to be removed *via in situ* oxidation by the active oxygen species from CeO₂, and the exposed HZSM-5 was tolerant to the chlorination of acid sites and avoided the direct adsorption of HCl on CeO₂. Additionally, the presence of water and ethyl acetate (EA) dramatically inhibited the activity of CeO₂@HZSM-5 for DCE oxidation, but water also completely suppressed the formation of PCHs by-products. The high Si/Al ratio could improve the water-resistance due to the increase of hydrophobicity, and the induction of trace Pd (0.1 wt%) further increased the CO₂ selectivity.

© 2016 Elsevier B.V. All rights reserved.

1. Introduction

Chlorinated volatile organic compounds (CVOCs), like 1, 2-dichloroethane (DCE), dichloromethane (DCM) and trichloroethylene (TCE), are considered as major contributors to air pollution due to their toxicity, the damage in the ozone layer and low bio-degradability. Among applicable disposal methods of CVOCs pollution, the low temperature catalytic total oxidation/combustion is a well-established and the most promising technology. However, the development of more efficient catalysts for the oxidation of CVOCs is key and challenging, and three types of catalysts such as supported noble metals, transition metal oxides and zeolites have been widely studied. Unfortunately, great efforts are still needed to be made to enhance catalytic activity, inhibit

the formation of highly chlorinated by-products and improve the stability of catalysts. Among them, the deactivation of catalysts is the general and trickiest problem that needs to be solved urgently. González-Velasco et al. [1] reviewed recently the main reasons leading to catalyst deactivation: (i) volatilization of the active phase, such as Cr-based catalysts; (ii) chlorine and/or hydrogen chloride poisoning, for example, bulk CeO₂ catalyst; (iii) thermal degradation/sintering, such as Ce/Zr mixed oxides and supported noble metal catalysts, and (iv) formation of coke deposits, like H-zeolites.

Traditionally, H-zeolites have found extensive applications as solid acid catalysts in the petrochemical and refining industries. Besides, zeolite also has attracted special attention for the total oxidation of CVOCs in the past few years. González-Velasco research group [2,3] reported the oxidation of chlorinated alkanes and ethylenes over different H-type zeolites (such as H-Y, H-ZSM-5, H-BEA and H-MOR), and revealed that Brønsted acidity played a dominant role for the adsorption and activation of CVOCs, and

* Corresponding authors.

E-mail addresses: daiqg@ecust.edu.cn (Q. Dai), wangxy@ecust.edu.cn (X. Wang).

also inhibited significantly the selectivity to molecular chlorine (Cl_2) and polychlorinated hydrocarbons (PCHs) by-products. Moreover, the generation of strong acidity (for example, dealumination *via* ammonium hexafluorosilicate treatment) further enhanced the active performance of zeolites catalysts [5]. However, a rapid deactivation of the H-zeolite was found and exclusively associated to coking due to its strong acidity [6,7]. Although, catalytic activity of the deactivated catalysts commonly could be partially recovered by burning coke with oxygen, but this method usually occurred at high temperature and required an accurate control of temperature (since the combustion reaction is highly exothermic). For example, González-Velasco et al. [6] reported that the coke formed from DCE oxidation on H-BEA could only be fully removed at higher temperatures (500 °C), while the coke formed from TCE oxidation was only removed 33%. Additionally, the coke also could be inhibited partially by using zeolites with appropriate pore channel system. For example, H-MOR with only one-dimensional channels easily suffered the coking deactivation, however, H-BEA and H-ZSM-5 with the interconnected channels showed a higher stability for the oxidation of DCE [8]. Nonetheless, the complete inhibition of coke was unavailable. In recent years, the introduction of transition metals (such as Cr, Cu, Co and Mn) gained more attention, because it not only decreased significantly coke deposition on zeolites surface but also enhanced the catalytic activity and the CO_2 selectivity [9–11]. In particular, due to the outstanding redox properties, oxygen storage capacity and bulk CeO_2 revealed an incredible catalytic activity for catalytic total oxidation of CVOCs [12], the modification of CeO_2 on zeolites attracted special attentions [13–17]. González-Velasco et al. [13,14] reported that the catalytic oxidation of DCE over $\text{CeO}_2/\text{HZSM-5}$ catalysts was promoted obviously due to the synergy between acid sites and oxygen mobility. Zhou et al. [15–17] also found the loading of CeO_2 generated a notable enhance for total oxidation of DCE over H-Y catalysts, and the synergy between CeO_2 species and Y zeolite was responsible for the enhancement of the catalytic activity. Moreover, they found that the addition of Cu or Cr as the second component could further improve the durability of CeO_2/Y catalysts due to the slight suppression of coke and the formation of more acid sites [18,19]. However, CeO_2 was easy to suffer the chlorine poisoning, which would cause the deactivation and the loss of oxidation ability [20]. Besides, CeO_2 (certainly, noble and transition metal oxides were also no exceptions) was identified as an excellent catalyst for the oxidation of HCl into Cl_2 (Deacon reaction) [21,22], which would promote the formation of more toxic poly-chlorinated by-products, especially at a higher temperature. Therefore, the coking/chlorine poisoning deactivation and the formation of chlorinated by-products are crucial for the design of CVOCs catalytic combustion catalysts.

In our previous work [23], we developed a simple and controlled method for preparing zeolite membrane on microscale sheet-like supports such as CeO_2 nanosheets, a novel $\text{CeO}_2\text{-ZSM-5}$ hybrid composite, namely CeO_2 nanosheets encapsulated by HZSM-5 particles (sandwich-structured $\text{CeO}_2@\text{HZSM-5}$). The hybrid materials present both distinct acidity and redox properties, and the exposure of CeO_2 is controlled, herein, is used to the catalytic total oxidation of CVOCs (DCE as a model molecule) to further understand and solve the coking of zeolites and chlorine poisoning of CeO_2 based catalysts. As a reference, $\text{CeO}_2/\text{HZSM-5}$ (CeO_2 dispersed on the surface of HZSM-5) and $\text{CeO}_2 + \text{HZSM-5}$ (CeO_2 physically mixed with HZSM-5) were prepared by incipient-wetness impregnation method and physically mixing method. The catalytic activity, products distribution, formation pathway of by-products, the stability (resistance to coking and chlorine poisoning deactivation) and the coke analysis were discussed, besides, the effect of water and ethyl acetate (EA) on catalytic activity, PCHs by-products and CO_2 selectivity also was studied.

2. Experimental

2.1. Catalysts preparation

2.1.1. Preparation of $\text{CeO}_2@\text{HZSM-5}$

The synthesis of $\text{CeO}_2@\text{HZSM-5}$ included two steps: the preparation of monodispersed CeO_2 nanosheets and the growth of dense ZSM-5 zeolite membranes. CeO_2 nanosheets were fabricated *via* a simple precipitation method at room-temperature and the same with the procedure reported earlier [24], and ZSM-5 membranes were prepared by an *in situ* two-step hydrothermal growth method under dynamic conditions [23]. Additionally, $\text{PdO-CeO}_2@\text{HZSM-5}$ also was prepared according to the Reference [23], but the mass loading of Pd was only 0.1%.

2.1.2. Preparation of $\text{CeO}_2/\text{HZSM-5}$ and $\text{CeO}_2 + \text{HZSM-5}$

For the purpose of comparison, $\text{CeO}_2/\text{HZSM-5}$ and $\text{CeO}_2 + \text{HZSM-5}$ were prepared by a traditional incipient-wetness impregnation method and physically mixing method, respectively. The detail procedures were as follows: HZSM-5 was impregnated by a certain concentration of $\text{Ce}(\text{NO}_3)_3 \cdot 6\text{H}_2\text{O}$ solution to obtain CeO_2 loading of 45 wt.%, and then the impregnated catalyst was dried at 110 °C and calcined at 450 °C for 4 h in air stream (100 ml/min). $\text{CeO}_2 + \text{HZSM-5}$ was directly prepared by mixing mechanically the synthesized CeO_2 nanosheets and HZSM-5 zeolite (grinding for 15 min in an agate mortar) and the mass fraction of HZSM-5 zeolite were 55 wt.%.

2.2. Catalysts characterization

The phase of all samples was analyzed by a Rigaku D/Max-rC X-ray diffractometer with Cu Ka radiation. The loadings of CeO_2 and Si/Al ratios were determined by X-Ray Fluorescence (XRF) analysis on Shimadzu XRF-1800. The BET surface area was measured on an ASAP 2400 system and all the samples were degassed at 160 °C for 2 h before testing. Scanning electron microscopy (SEM) images were performed on Hitachi S-3400N electron microscopes. Hydrogen temperature programmed reduction ($\text{H}_2\text{-TPR}$) and temperature programmed desorption of NH_3 ($\text{NH}_3\text{-TPD}$) were carried out on a homemade quartz micro-reactor, and the detail procedures referred to the Reference [25].

2.3. Catalytic activity tests

Catalytic oxidation of 1, 2-dichloroethane as a model reaction of CVOCs combustion was tested in a U-shaped quartz tube reactor (I. D. = 3 mm), 100 mg of catalyst (60–80 mesh) was used in each experiment and the feed stream containing 1000 ppm of DCE and Air balance gas was passed through the catalyst bed at 50 ml/min (30,000 ml/h_{gcat}). The reactants and chlorinated by-products were analyzed by an on-line FID gas chromatograph, the KB-5 capillary column was used and the column temperature was set to 40 °C to the separation of chlorinated products, especially for E-dichloroethene and Z-dichloroethene. The concentration of CO was determined by using a CO gas-detector and the selectivity was calculated to evaluate the oxidation performance of catalysts. Water steam (5 v/v%) was introduced into the reaction system through a temperature controlled bubbler, ethyl acetate (EA, 500 ppm) mixed with DCE and was injected into a vaporizer by a syringe pump (KD Scientific, KDS-101). Additionally, all pipes were heated by electricity and maintained at 120 °C to ensure the complete vaporization of DCE and water/EA.

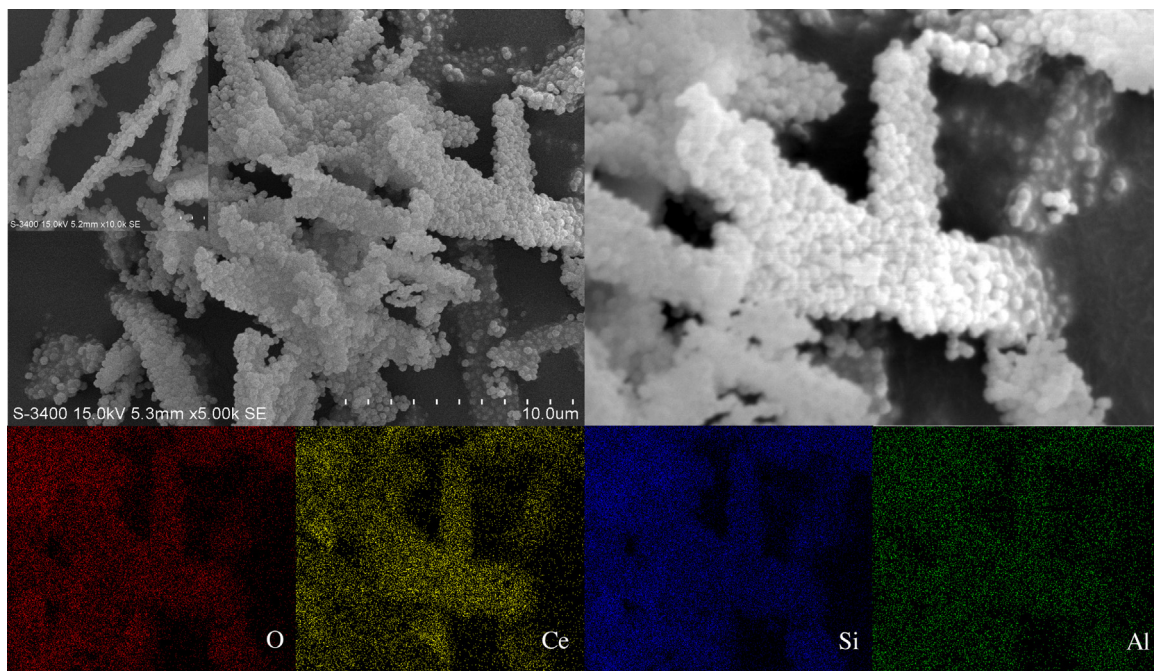


Fig. 1. Typical SEM images and EDX elemental mappings of $\text{CeO}_2@\text{HZSM-5}$.

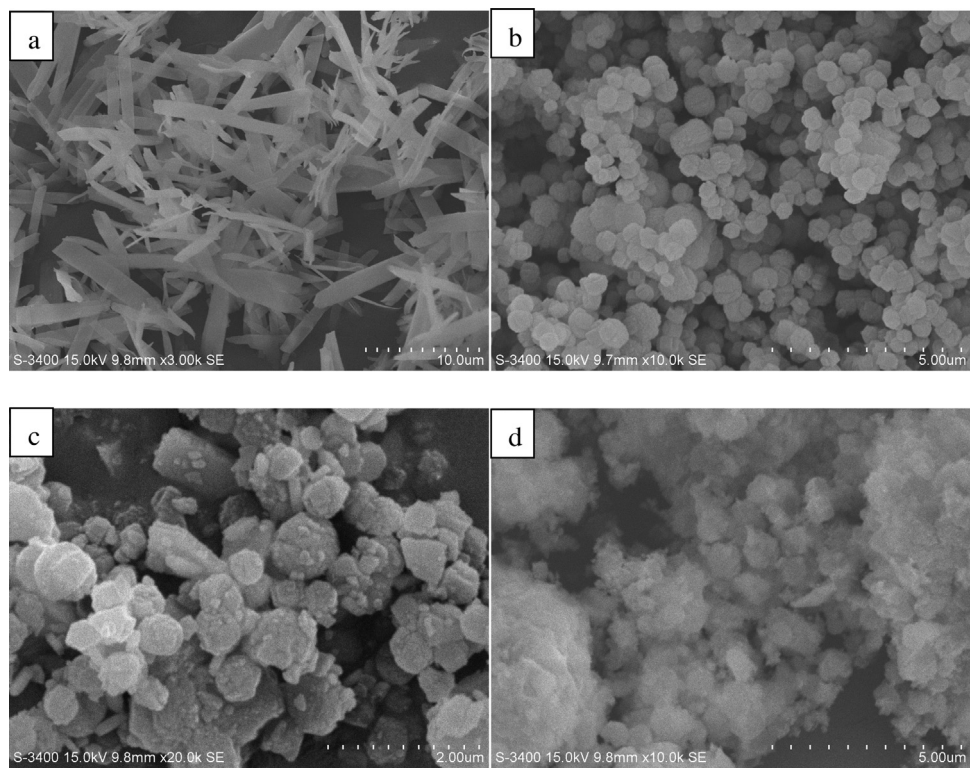


Fig. 2. Typical SEM images of CeO_2 (a), HZSM-5 (b), $\text{CeO}_2 + \text{HZSM-5}$ (c), and $\text{CeO}_2/\text{HZSM-5}$ (d).

2.4. Coke analysis

2.4.1. Temperature programmed oxidation (TPO)

The temperature programmed oxidation (TPO) of the spent catalysts (after stability tests at 250 or 350 °C for 8 h) was carried out in a U-type quartz tube. The catalysts were heated from 100 to 650 °C in 30 ml/min O_2 flow at a heating rate of 10 °C/min, and CO and CO_2 were monitored on-line by a mass spectrometer apparatus (HIDEN

HPR-20). Additionally, the evolution of HCl and Cl_2 adsorbed on the surface of catalysts was also detected.

2.5. Raman and XPS spectra

To further understand the type of coke, Raman and XPS spectra of the spent catalysts (after stability tests at 250 °C for 8 h) were carried out on an inVia + Reflex (Renishaw) Raman spectrom-

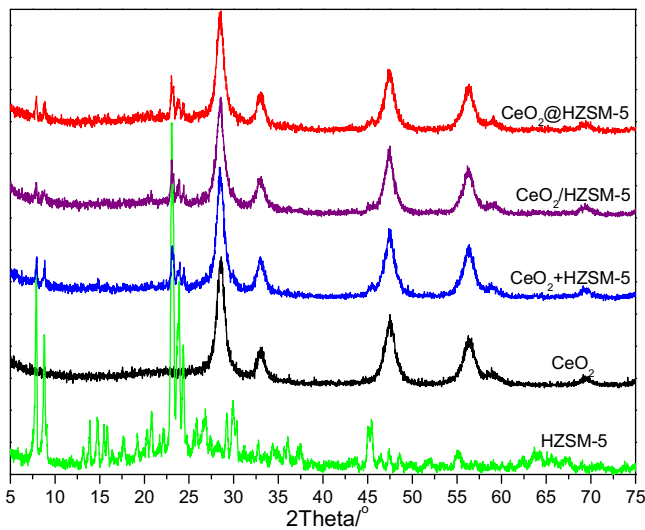


Fig. 3. XRD patterns of the CeO_2 -HZSM-5 composite catalysts.

eter and an ESCALAB 250Xi (Thermo Fisher) X-ray photoelectron spectrometer, respectively.

3. Results and discussion

3.1. Characterization

Fig. 1 showed typical SEM images of CeO_2 @HZSM-5 composite and EDX elemental mappings, as reference, SEM images of CeO_2 , HZSM-5, $\text{CeO}_2 + \text{HZSM-5}$ and $\text{CeO}_2/\text{HZSM-5}$ catalysts also were presented in Fig. 2. The SEM images (Fig. 1) indicated that all surfaces of CeO_2 nanosheet including the cross sections were encapsulated by a monolayered spherical particles (a diameter of 200–400 nm), notably, these particles arranged continuously and densely in the form of membranes (for more SEM images, see Fig. S1) formed by means of the reaction between the hydrolyzed TEOS (Si-OH or hydroxy groups of Si-O-Si condensates) or ZSM-5 nutrients and the surface hydroxy groups of CeO_2 with high reactivity, which was consistent with our previous report [23]. In brief, CeO_2 @HZSM-5 composite demonstrated a sandwich-like core-shell structure, and CeO_2 surfaces were coated completely and not directly exposed to the environment. Additionally, the EDX elemental mappings revealed that the Si and Al elements were well dispersed on the CeO_2 surface and displayed a same sheet-like structure with CeO_2 nanosheets.

As shown in Fig. 2, pure CeO_2 was composed of a large amount of uniform and monodispersed nanosheets (ca. 5–10 μm in length and about 0.5–1.2 μm in width) [24], the prepared pure HZSM-5 sample was hierarchical microspheres and these spheres were about 550–750 nm in diameter, and the external surface of the spheres was consisted of aggregated and interconnected nanorod-like crystals (mixed with a small amount of intergrowing crystals, which was confirmed by TEM) [26]. Additionally, it can be found that the sizes of ZSM-5 particles decreased from 550 to 750 nm to 200–400 nm for CeO_2 @ZSM-5 possible due to the confinement effects of CeO_2 supports on ZSM-5 crystals growth. For the $\text{CeO}_2 + \text{HZSM-5}$ prepared by physically mixing method, HZSM-5 still presented the primary morphology, whereas CeO_2 nanosheets were broken into small and irregular pieces and most of them covered on the surface of ZSM-5 particles. $\text{CeO}_2/\text{HZSM-5}$ displayed a similar morphology with HZSM-5 particles, but the surface of ZSM-5 was almost completely encapsulated by cottony CeO_2 particles.

Fig. 3 showed XRD patterns of three CeO_2 -HZSM-5 composite samples, bulk CeO_2 and HZSM-5 catalysts. For all the CeO_2 -HZSM-

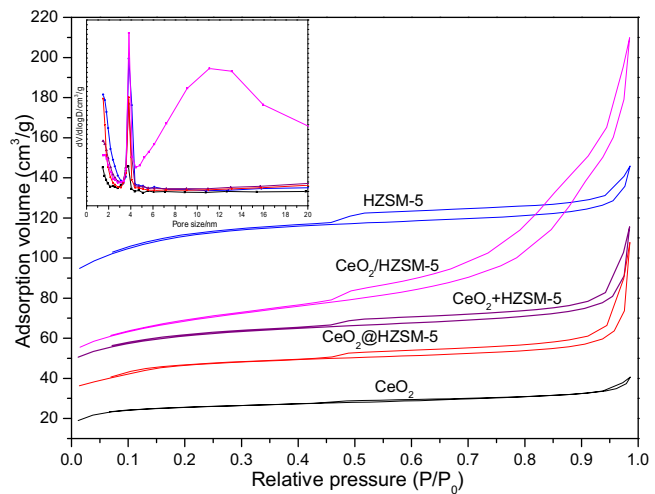


Fig. 4. The N_2 adsorption-desorption isotherms and pore size distribution curves of CeO_2 -HZSM-5 composite catalysts.

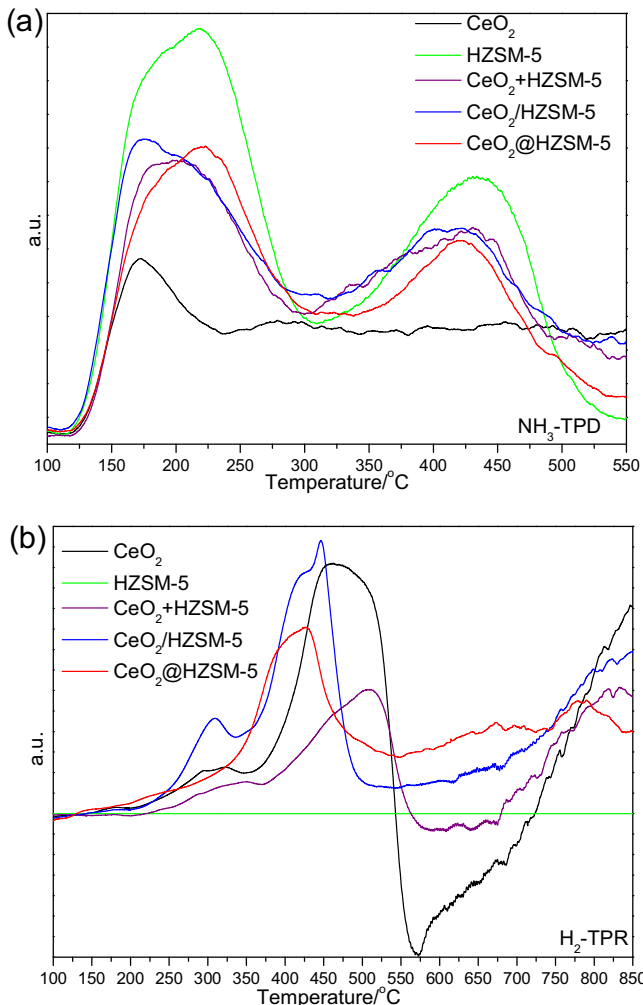
5 composite catalysts, the peaks corresponding to CeO_2 with a fluorite-like structure (JCPDS 89-8436, at $2\theta = 28.6^\circ, 33.1^\circ, 47.5^\circ$ and 56.4°) and ZSM-5 with a MFI type framework (JCPDS 44-0003, at $2\theta = 7.9^\circ, 8.8^\circ, 23.0^\circ, 23.9^\circ, 29.8^\circ, 45.5^\circ$ and 55.1°) could be clearly observed. The mean crystallite size of CeO_2 , calculated based on the X-ray line broadening of the (111) peak of ceria using the Scherrer equation, remained at a similar size of about 7.8 nm. Additionally, XRF results (Table 1) showed that the ceria content of the CeO_2 @HZSM-5 sample was 45 wt.%, and the Si/Al ratio was 75 and higher than that pure HZSM-5 (Si/Al = 54), which indicated that the presence of CeO_2 was not favored to the introduction of Al. The ceria content of the $\text{CeO}_2/\text{HZSM-5}$ and $\text{CeO}_2 + \text{HZSM-5}$ samples was 47 wt.% and 45 wt.%, respectively.

The N_2 adsorption-desorption isotherms and BJH pore size distributions were shown in Fig. 4, and Table 1 also summarized the textural properties (such as BET surface area and pore volume/size) of all the samples. The pure HZSM-5 sample presented a Type IV isotherm and was typical for mesoporous materials, and the hysteresis loop in a relative pressure (P/P_0) range between 0.45 and 0.9 illustrated the presence of irregular mesopores from agglomeration of particles [3,4], which was in good agreement with the structure of hierarchical microspheres observed by SEM, and the pore size distributions suggested that the sample had a mesopore size centered at about 4 nm. However, it's pointed out that Groen considered that the peaks at 2 and 4 nm in the pore size distribution strictly associated with the nature of the adsorbed phase (especially for MFI-type zeolites), not physical mesopores [27]. All CeO_2 based samples also exhibited an additional steep uptake in higher relative pressure ranges ($P/P_0 > 0.95$) besides a similar hysteresis loop with pure HZSM-5, which corresponded to the macropores formed by the accumulation of CeO_2 primary nanoparticles. In contrast, $\text{CeO}_2/\text{HZSM-5}$ possessed more and larger macropores, a larger mesopore at about 13 nm besides a possible mesopore at about 4 nm (with an average mesopore size of 6 nm), owing to the accumulation of CeO_2 nanoparticles.

The NH_3 -TPD and H_2 -TPR of CeO_2 -HZSM-5 composites were illustrated in Fig. 5 to evaluate the acid and redox properties of these samples. As shown in Fig. 5a, all the samples except pure CeO_2 exhibited two ammonia desorption peaks at about 220 and 450 $^\circ\text{C}$, which corresponded to the weak and strong acid sites of HZSM-5, while the pure CeO_2 only displayed one small peak in the range of low temperature (Peak Temp at about 175 $^\circ\text{C}$), which was indicative of less acid number and weak acid strength. Additionally, it can be found that the presence of CeO_2 caused a

Table 1Physico-chemical properties of CeO_2 -HZSM-5 composite catalysts.

Samples	S_{BET} (m^2/g)	Average Pore size(nm)	Pore Volume(cm^3/g)	Crystallite size (nm)	XRF	
					Si/Al	CeO_2 (wt%)
CeO_2	78	3.2	0.06	7.9	–	100
HZSM-5	335	2.7	0.23	–	54	0
$\text{CeO}_2 + \text{HZSM-5}$	187	3.8	0.18	7.8	54	45
$\text{CeO}_2/\text{HZSM-5}$	216	6.0	0.32	7.2	54	47
$\text{CeO}_2@\text{HZSM-5}$	171	4.2	0.18	7.8	75	45

**Fig. 5.** NH_3 -TPD (a) and H_2 -TPR (b) profiles of CeO_2 -HZSM-5 composite catalysts.

slight decrease of acid strength, especially for the weak acid sites of $\text{CeO}_2/\text{HZSM-5}$ and $\text{CeO}_2 + \text{HZSM-5}$ samples (namely the samples exposed CeO_2), moreover CeO_2 -HZSM-5 composite catalysts exhibited almost the same total amount of acidity due to the same content of HZSM-5. The H_2 -TPR profiles (Fig. 5b) indicated that two peaks were observed at 225–350 °C (α peak) and 510 °C (β peak) over pure CeO_2 sample, which attributed to the reduction of the surface oxygen species adsorbed on oxygen vacancies and the surface lattice oxygen (the uppermost layers of Ce^{4+}), respectively. Moreover, the H_2 consumption above 600 °C was ascribed to the reduction of bulk lattice oxygen. Note that no detected H_2 consumption was observed for the pure HZSM-5 zeolite due to the absence of reducible oxygen species. For the $\text{CeO}_2@\text{HZSM-5}$ and $\text{CeO}_2/\text{HZSM-5}$ catalysts, the Peak Temp of the β peak obviously shifted to the lower temperature (decreased from 510 °C to about 430 °C), whereas the reduction temperature range of $\text{CeO}_2 + \text{HZSM-5}$

5 was identical to that of pure CeO_2 . This showed, the shift of β peak to lower temperature was an indication of the strong interaction between CeO_2 and HZSM-5 for the first two, while only physical contact between CeO_2 and HZSM-5 was present in $\text{CeO}_2 + \text{HZSM-5}$ sample prepared by physically mixing method. Moreover, the α peak of $\text{CeO}_2@\text{HZSM-5}$ disappeared, which confirmed that the surface of CeO_2 was completely encapsulated by ZSM-5 particles and the dissociative adsorption of gaseous oxygen on CeO_2 was inhibited. Expectedly, the $\text{CeO}_2/\text{HZSM-5}$ displayed the largest hydrogen consumption of α peak due to the high dispersion of CeO_2 on HZSM-5.

These series of characterizations (SEM and H_2 -TPR) showed that the CeO_2 -HZSM-5 composite catalysts with different morphologies, redox performances and exposure states of CeO_2 could be prepared by controlled methods. More specifically, $\text{CeO}_2@\text{HZSM-5}$ synthesized by *in situ* hydrothermal growth method displayed a sandwich-like core-shell structure and CeO_2 was encapsulated by HZSM-5, whereas $\text{CeO}_2/\text{HZSM-5}$ sample was just the opposite. For the $\text{CeO}_2 + \text{HZSM-5}$ sample, both CeO_2 and HZSM-5 was open and exposed. The first two of these revealed the strong interaction between CeO_2 and HZSM-5, whereas only physical interaction was observed for $\text{CeO}_2 + \text{HZSM-5}$. Moreover, more importantly, the significant differences of the acid properties (acid strength and total acidity) were not detected among these three composite catalysts. Therefore, these well designed CeO_2 -HZSM-5 composite catalysts made it possible to systematically study the roles of CeO_2 and HZSM-5, and to more deeply understand the synergistic effect between CeO_2 and HZSM-5 for the resistant to coking and chlorine poisoning in catalytic oxidation of CVOCs by eliminating the effects of acid properties as the active sites of H-typed zeolites.

3.2. Catalytic activity, product distribution and stability

Fig. 6 showed the conversion curves of DCE oxidation over the CeO_2 -HZSM-5 composite catalysts and the corresponding concentration of vinyl chloride (VC) as the main chlorinated by-product, and the curves of pure CeO_2 and HZSM5 also were presented as a comparison. As shown in Fig. 6, the conversion vs temperature plot of DCE over the pure CeO_2 catalyst exhibited a flat in the lower temperature range (175–250 °C) and the 90% conversion was only achieved at 350 °C, meanwhile, the conversion increased continuously with the increase of temperature during oxidation processes of low concentration DCE (500 ppm) and the conversion flat was not observed, which was the indication of chlorine poisoning deactivation due to the accumulation of HCl from the oxidation of high concentration DCE on the surface active sites of CeO_2 [20]. The introduction of HZSM-5, such as $\text{CeO}_2 + \text{HZSM-5}$ and $\text{CeO}_2/\text{HZSM-5}$ catalysts, apparently inhibited the deactivation and the flat of conversion curves disappeared, thus, the conversion of DCE over these two catalysts was significantly higher than pure CeO_2 , especially at high temperature ranges (namely the latter stages of activity tests). However, as with pure CeO_2 catalyst, the CeO_2 component of these two catalysts also was completely exposed and directly contacted with DCE molecules, in principle, inorganic chlorine species also would adsorb on active sites of CeO_2 and caused the chlorine poi-

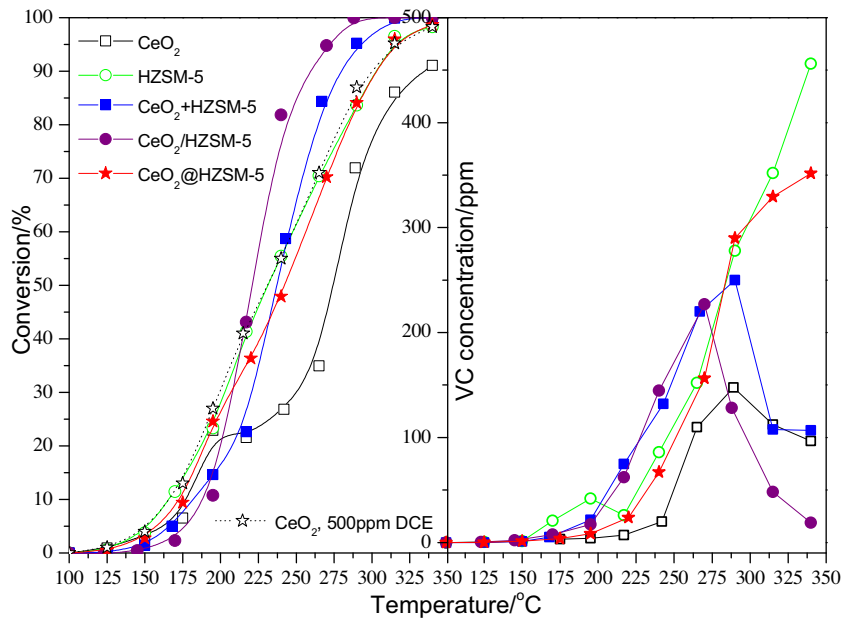


Fig. 6. The light-off curves of the CeO_2 -HZSM-5 composite catalysts and the corresponding concentration of vinyl chloride (VC) as the main by-product.

sioning deactivation. Hereby, it can be speculated that the inhibition of chlorine poisoning should be ascribed to HZSM-5 or synergistic effect of HZSM-5 and CeO_2 which promoted the rapid removal of HCl from the surface or active sites of CeO_2 . For example, the formation of HCl occurred primarily on HZSM-5 *via* the abstraction of HCl on acidity sites and the main role of CeO_2 was to completely oxidize the dissociated DCE. Furthermore, CeO_2 /HZSM-5 presented a better catalytic activity for the DCE oxidation comparing with CeO_2 + HZSM-5, which was ascribed to the strong interaction between CeO_2 and HZSM-5 (H₂-TPR results). HZSM-5 and CeO_2 @HZSM-5 catalysts displayed an almost overlapping light-off curve and a lower catalytic activity than the catalysts with exposed CeO_2 (CeO_2 /HZSM-5 and CeO_2 + HZSM-5). Generally, solid acid catalysts (such as H-type zeolites) presented a lower activity for total oxidation of CVOCs due to the more difficult dissociation of the C-Cl bonds on acid sites and the absence of oxidation ability compared with noble metal or transition metal catalysts [13–17]. This result also indicated that CeO_2 was not involved directly in the adsorption and activation or dissociation of DCE for the oxidation of DCE over CeO_2 @HZSM-5 catalyst and HZSM-5 was the main active phase (DCE oxidation occurred based on acid catalysis pathway), and further confirmed that CeO_2 was coated completely by HZSM-5. Additionally, the concentration cures of vinyl chloride (VC) as the main by-product revealed that the catalysts with the exposed CeO_2 , including pure CeO_2 , CeO_2 + HZSM-5 and CeO_2 /HZSM-5, displayed a maximum value at about 275–300 °C, while HZSM-5 and CeO_2 @HZSM-5 catalysts showed a continuously rising trend with the increase of reaction temperature. This is mainly due to the fact that CeO_2 exhibited a better activity for the subsequent oxidation of VC than HZSM-5. Additionally, the concentration of VC over CeO_2 + HZSM-5 and CeO_2 /HZSM-5 was higher than pure HZSM-5 or CeO_2 below 275 °C, which was attributed to the high activity, the synergistic effect of HZSM-5 and CeO_2 or the reduction of the protonic acid sites [15], while the slight less formation of VC over CeO_2 @HZSM-5 at a higher temperature compared with HZSM-5 was mainly due to the good oxidation performance and high activity for VC oxidation of CeO_2 located below the HZSM-5 particles.

Furthermore, Fig. 7 presented the distribution profiles of other chlorinated by-products (not including VC) vs reaction temperature, notably, all by-products were identified by GC-MS *via* the

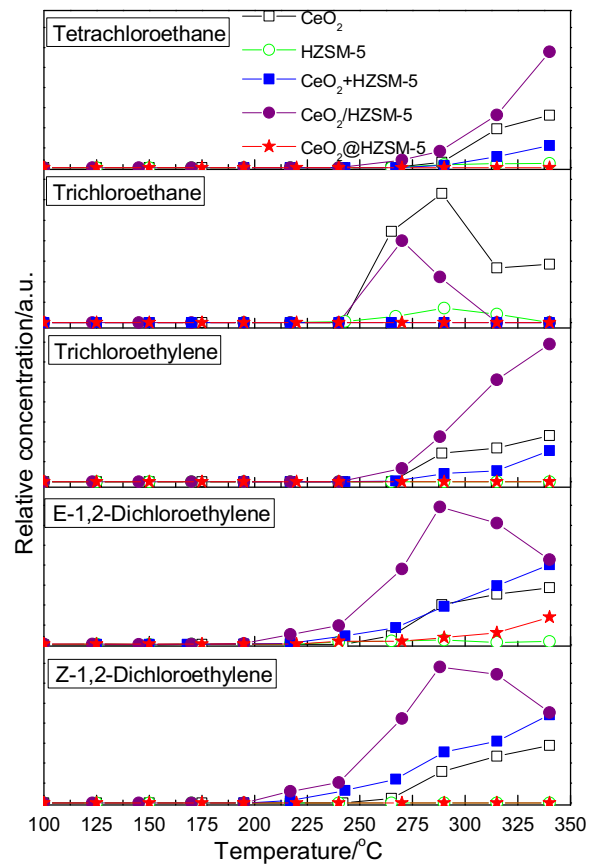
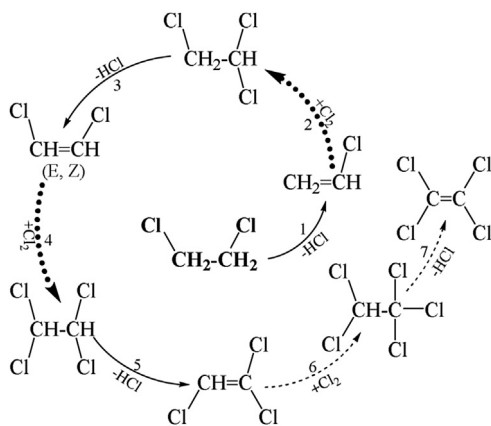


Fig. 7. Concentration curves of by-products (not including VC) over CeO_2 -HZSM-5 composite catalysts.

effluent gases were absorbed in 1, 2-dichloroethane liquid. For pure CeO_2 , CeO_2 /HZSM-5 and CeO_2 + HZSM-5 catalysts, namely catalysts with the exposed CeO_2 component, additional five chlorinated hydrocarbons were observed, including 1, 2-dichloroethene (E and Z), trichloroethylene, 1, 1, 2-trichloroethane and tetrachloroethane. It should be noted that these by-products were



Scheme 1. The formation pathways of chlorinated by-products during 1, 2-dichloroethane oxidation over CeO_2 -HZSM-5 composite catalysts.

formed only in very low concentrations. Whereas, these by-products over pure HZSM-5 and CeO_2 @HZSM-5 was not detected or negligible. Thus, it can be speculated that the formation of these by-products was related to the exposed CeO_2 component. Additionally, it can be found that the formation temperature of these chlorinated by-products was different, but each of them formed at almost the same temperature for the three different catalysts. Combined with Fig. 6, the VC was first observed over all investigated catalysts and initially formed at 175°C , which was ascribed to the dehydrochlorination of 1, 2-dichloroethane on acidic or basic sites. Next, E-dichloroethene and Z-dichloroethene were detected simultaneously (at 225°C), which corresponded to the dehydrochlorination of 1, 1, 2-trichloroethane with different conformation through a concerted elimination mechanism [28]. However, 1, 1, 2-trichloroethane was only observed above 250°C , which might be due to the low concentration and sensitivity, and the same concentration trend of these three products (the maximum value was achieved at about 300°C) also conformed the formation of 1, 2-dichloroethene via the dehydrochlorination of 1, 1, 2-trichloroethane. Additionally, the formation of 1, 1, 2-trichloroethane was considered to be related to the formation of chlorine (our previous work indicated that CeO_2 presented an evident activity for Deacon reaction at higher temperature [29]) and the subsequent chlorination reactions of VC. With the increase of the reaction temperature, trichloroethylene and tetrachloroethylene were formed (at about 275°C) and showed a same trend of concentration vs reaction temperature. These poly-chlorinated by-products formed via a sequential dehydrochlorination and chlorination pathway as indicated in Scheme 1. Notably, pentachloroethane and tetrachloroethylene (steps 6 and 7) were not detected under our experimental conditions, it was probably because they occurred only at higher temperature. Although, the formation temperature of these by-products over different catalysts was almost the same, the concentration of them were considerably different and depended on the used catalysts. In brief, CeO_2 -HZSM-5 demonstrated a maximum concentration of all these by-products except 1, 1, 2-trichloroethane (pure CeO_2 showed a maximum concentration due to the better activity for Deacon reaction), which was due to the strong interaction and the synergistic effect between CeO_2 and HZSM-5.

Fig. 8 showed the conversion of DCE over CeO_2 -HZSM-5 composite catalysts with time-on-stream at 250°C for 8 h. Pure HZSM-5 and CeO_2 catalysts both presented a rapid decline in conversion during the initial stages of the reactions, by comparison, the deactivation of CeO_2 was more evident and the conversion decreased from 70 to 30% within 30 min. This deactivation was predictable, because numerous studies had shown that coking and chlorine

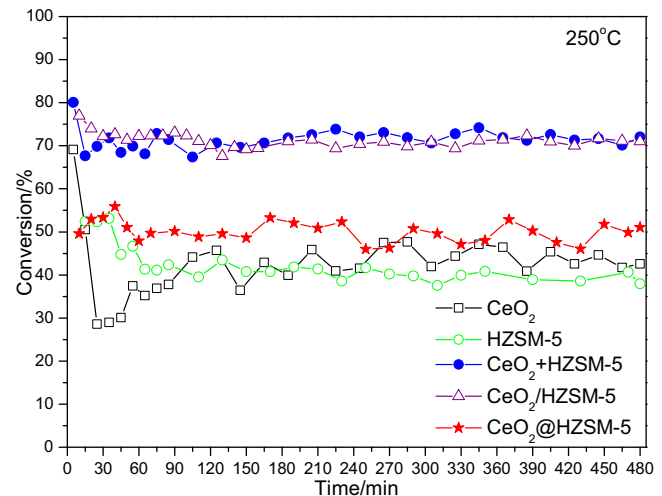


Fig. 8. Catalytic activity of CeO_2 -HZSM-5 composite catalysts as a function of time-on-stream at 250°C (1000 ppm and 30,000 ml/h gcat).

poisoning caused the rapid deactivation of HZSM-5 and CeO_2 [6,15,20], respectively. Along with the prolonging of reaction time (after 60 min), a gradual decrease in conversion was observed over HZSM-5 catalyst due to the slow accumulation of coke. Conversely, CeO_2 catalyst revealed an increased DCE conversion owing to the partial chlorination of surface CeO_2 was beneficial to the dehydrochlorination of 1, 2-dichloroethane to vinyl chloride, which was confirmed by the increase of VC selectivity. For CeO_2 -HZSM-5 and CeO_2 + HZSM-5 catalysts, the conversion of DCE fell rapidly but slightly during the initial 30 min interval and then tended to remain reasonably stable at longer time-on-stream. This behavior also was observed in the total oxidation of DCE on CeO_2 /ZSM-5 and CuO/CeO_2 /USY zeolite catalysts reported by de Rivas and Huang [13,18]. However, we inferred that the declined activity was from the loss of activity corresponding to the isolated CeO_2 due to chlorine poisoning, while the inhibition or elimination of the coke benefiting from CeO_2 and the removal of HCl owing to HZSM-5 synthetically made the excellent stability. Significantly, an appreciable deactivation of CeO_2 @HZSM-5 was not observed during the stability tests, thus the coking and chlorine poisoning deactivation were avoided. But, the conversion displayed a slight oscillation between 55% and 50%, which possibly indicated that the formation of coke still occurred over CeO_2 @HZSM-5 catalyst, while the formed coke can be oxidized *in situ* due to the better oxidizing ability of CeO_2 located below ZSM-5 particles. To further understand the oxidation and coking behaviors of DCE on CeO_2 -HZSM-5 composite catalysts, the spent catalysts were investigated via various techniques.

3.3. Coke analysis

Fig. 9 presented TPO profiles of the spent catalysts, after the stability tests at 250°C for 8 h, to evaluate the formation of coke and the adsorption/desorption or transformation of HCl/Cl₂ on the catalysts surface. Over pure CeO_2 , an apparent desorption of HCl and formation of Cl₂ were observed above 375°C , which implied that the adsorption of HCl occurred on CeO_2 surface during the stability tests, and the adsorbed HCl could be oxidized to Cl₂ via a Deacon reaction pathway at higher temperature. Meanwhile, only weak MS signals of CO and CO₂ corresponding to the oxidation of coke were monitored. These results confirmed the deactivation of CeO_2 was mainly attributed to the accumulation of HCl on surface while the coking deactivation was negligible, and the oxidation of adsorbed HCl into Cl₂ led to the formation of polychlorinated by-product such as 1, 1, 2-trichloroethane. Additionally,

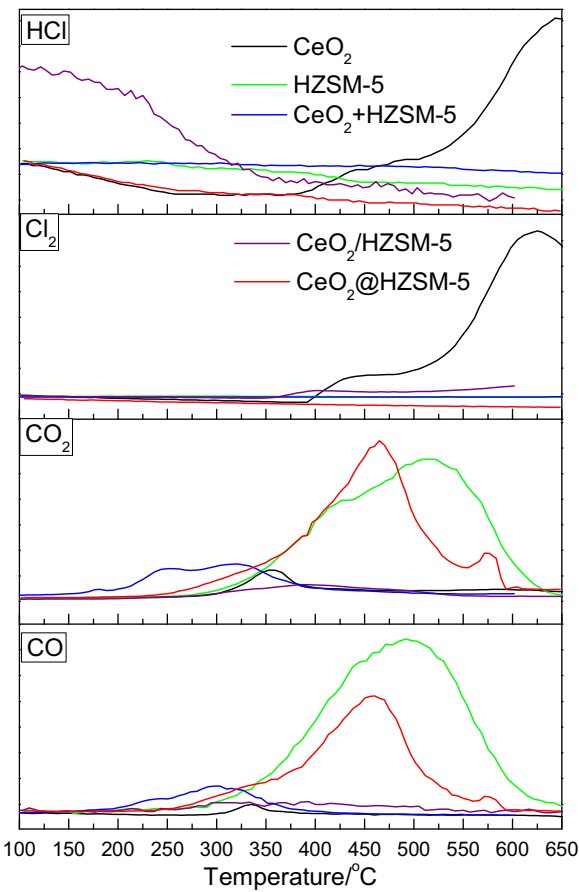


Fig. 9. TPO profiles of the spent catalysts (1000 ppm and 30,000 ml/h•gcat, at 250 °C for 8 h).

all ZSM-5 based catalysts did not exhibit a notable evolution of HCl and Cl₂, except the formation of trace amounts of Cl₂ over CeO₂/HZSM-5, which indicated that the formation/adsorption of HCl tended to occur on HZSM-5 composition while the removal of HCl on HZSM-5 surface was rapid, thus the deactivation owing to chlorine poisoning was slight or negligible. However, there was a significant difference in coking behavior among these catalysts. CeO₂/HZSM-5 catalyst displayed a neglected coke compared with CeO₂ + HZSM-5, CeO₂@HZSM-5 and HZSM-5 catalysts (CeO₂/HZSM-5 < CeO₂ + HZSM-5 < CeO₂@HZSM-5 < HZSM-5), and which was ascribed to the outstanding redox performance (H₂-TPR results), thus, the better stability of these two catalysts benefited from the low levels of coking and HCl adsorption. Although, the TPO results suggested that the coking also occurred on CeO₂@HZSM-5 during the stability test, the amount of coke was less and more coke could be oxidized directly into CO₂ (not CO) during TPO experiment compared with pure HZSM-5. Moreover, the initial oxidation temperature of the coke decreased from 350 °C to 225 °C. These results suggested that the coke deposited on CeO₂@HZSM-5 could be oxidized *in situ* due to the good redox performance of CeO₂ but was a slow process due to the slow migration of oxygen species presenting on CeO₂ encapsulated by HZSM-5, which was responsible for the excellent stability of CeO₂@HZSM-5 with a slight oscillation.

Fig. 10 also presented stability test of CeO₂@HZSM-5 at higher temperature (350 °C) and TPO profiles of the spent catalyst. A stable conversion of DCE (99%) was observed and the slight oscillation of conversion also disappeared, meanwhile, TPO profiles showed that the adsorption/accumulation of HCl on CeO₂@HZSM-5 surface did not occur during stability test and the formation of coke also was ignored. This showed that CeO₂@HZSM-5 catalyst displayed a

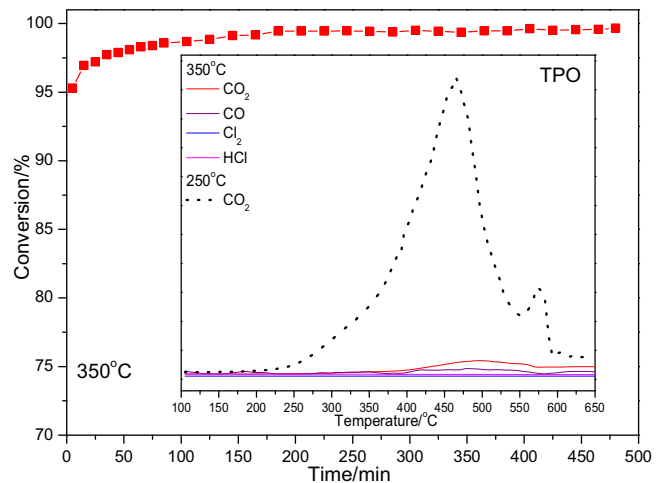


Fig. 10. Stability test of CeO₂@HZSM-5 at 350 °C and TPO profiles of the spent catalyst (1000 ppm and 30,000 ml/h•gcat, at 350 °C for 8 h).

superior resistance to coking and chlorine poisoning deactivation at a higher temperature (the temperature required in a practical application to achieve the complete oxidation of DCE) and was a promising catalyst.

Furthermore, natures of coke deposited on CeO₂@HZSM-5 during stability tests at 250 °C (pure HZSM-5 also was studied for comparison) was further analyzed by Raman and XPS techniques to better understand the oxidation behavior of DCE on CeO₂@HZSM-5 catalyst and the role of CeO₂, and the spectra were presented in Fig. 11. As shown in Fig. 11a, two distinct Raman bands at 1456 and 1605 cm⁻¹ were detected on both the spent HZSM-5 and CeO₂@HZSM-5. The former were assigned to paraffinic and cyclopentadienyl species (α , coke-type I or white coke), and the latter was attributed to polyolefinic and/or polyaromatic species (β , coke-type II or black coke) [30,31]. However, the intensity of these bands on HZSM-5 was greater than that of CeO₂@HZSM-5, which indicated that the amount of coke was more and consistent with the TPO results. More importantly, the α/β ratio value of CeO₂@HZSM-5 was larger compared with HZSM-5, indicating that the coke deposited on CeO₂@HZSM-5 was more disordered and amorphous. Stair proposed that the coke formed through the cyclopentadienyl intermediate species for a pure zeolite (metal-free) catalyst, and this species was thermally unstable and easily to be removed by oxidation [30], which was one of the key reasons why CeO₂@HZSM-5 exhibited a superior resistance to coking deactivation. Additionally, another band at 1148 cm⁻¹ was observed on pure HZSM-5 catalyst and assigned to bidentate carbonate species, which was an indication of weak redox ability. The presence of coke was also revealed by the XPS spectrum at C1s region (Fig. 11b), and four peaks at 283.5, 284.6, 285.9 and 288.6 eV could be observed on both HZSM-5 and CeO₂@HZSM-5 catalysts. Coke formation and coke species were studied by the XPS technique in CO₂ reforming of CH₄ on nickel-based catalysts [32], and several main coke species (such as carbonization, the carbonaceous contaminants in the vacuum system, non-activated charcoal and surface carbonate) existed on the surfaces of catalysts were detected, which binding energy was about 282, 284, 286, and 288 eV, respectively. It was considered that the surface carbonization and non-activated charcoal species (at 282 and 286 eV) was the main coke species and resulted in the deactivation of catalysts. Compared with the pure HZSM-5 catalyst, the coke species over CeO₂@HZSM-5 with a binding energy near 282 and 286 eV were suppressed, especially the non-activated coke species (286 eV), which interpreted that CeO₂@HZSM-5 exhibited a better resistance to carbon deposition and better stability.

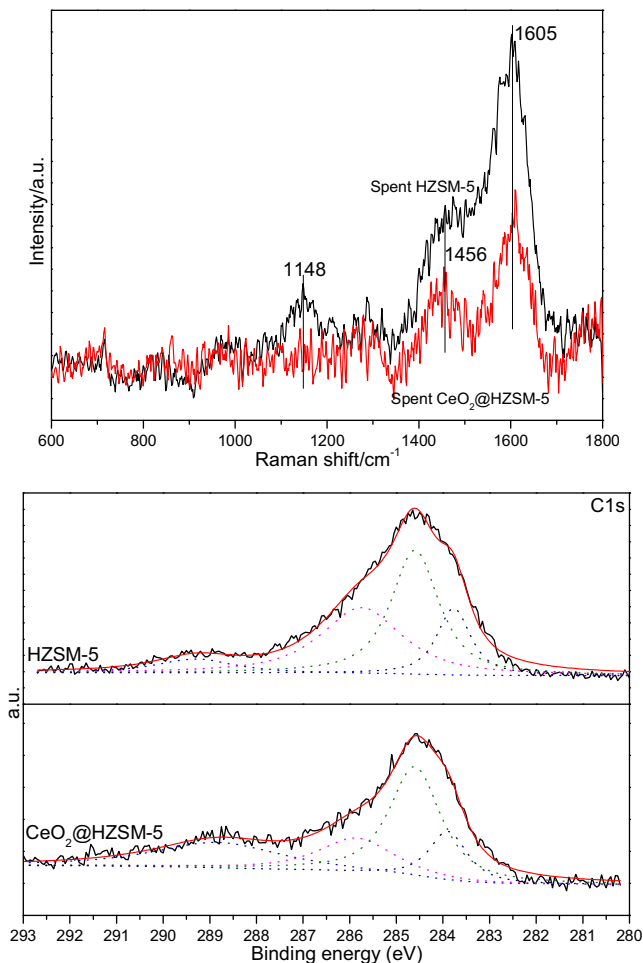


Fig. 11. Raman and XPS spectra of the spent HZSM-5 and CeO₂@HZSM-5 (1000 ppm and 30,000 ml/h•gcat, at 250 °C for 8 h).

3.4. Effect of H₂O and ethyl acetate

For the practical application of catalytic combustion for CVOCs elimination, the real exhaust condition was usually complicated

and harsh, for example, coexisting with high concentration of water and other non-chlorinated VOCs. Hence, the performance of CeO₂-HZSM-5 composite catalysts was evaluated under the reaction conditions with 5 vol.% of water or 500 ppm ethyl acetate (EA). **Fig. 12** presented the effect of H₂O (5 vol.%) on the conversion of DCE and CO selectivity, and chlorinated by-products were also analyzed and listed. The significant influences were observed, the T₅₀ (the temperature for 50% conversion of DCE) of pure CeO₂, CeO₂/HZSM-5 and CeO₂ + HZSM-5 increased by 25–30 °C in the presence of 5 vol.% H₂O, while the impact on the pure HZSM-5 and CeO₂@HZSM-5 was more noticeable (T₅₀, with an increase by 45–55 °C) and the conversion of DCE was only about 90% even at 350 °C. The decrease of activity was unsurprising due to the competitive adsorption between H₂O and DCE molecules on active sites [3]. However, the catalysts with exposed CeO₂ demonstrated better water resistance compared with HZSM-5 and CeO₂@HZSM-5, which could be attributed to the fact that CeO₂ was slightly hydrophobic (the weak affinity for water) [33], while the strong Brønsted acid sites of HZSM-5 could be destroyed in the presence of water [34] and the ZSM-5 with low Si/Al ratio (such as below 100) was hydrophilic. Our previous work [35] also indicated that water was more influential for the catalysts that Brønsted acid was considered as active sites, and pure CeO₂ was less affected. Additionally, the results from CO_x quantitative analysis showed that the CO selectivity of all catalysts was below 25% under dry condition, while the presence of H₂O increased evidently CO selectivity (up to about 50%) except that the rise of pure HZSM-5 and CeO₂ catalysts was almost negligible. Thus, it can be inferred that the formation of more CO under humid condition was the result of the synergies between CeO₂ and HZSM-5. Most importantly, chlorinated by-products except VC were completely inhibited when H₂O was introduced into the reaction system, even for VC, the maximum concentration also decreased from 250 to 450 ppm (without H₂O) to 20–35 ppm (5 vol.% H₂O). Specifically, three catalysts exposed CeO₂ under dry condition presented a less VC than pure HZSM-5 and CeO₂@HZSM-5 catalysts, which was related to the higher activity of CeO₂ for the oxidation of VC by-product (confirmed by the fact that the concentration of VC showed a maximum value vs temperature), while the inhibition of H₂O to the formation of VC on the latter two catalysts was sharper and even VC was not detected over CeO₂@HZSM-5 catalyst during the whole activity

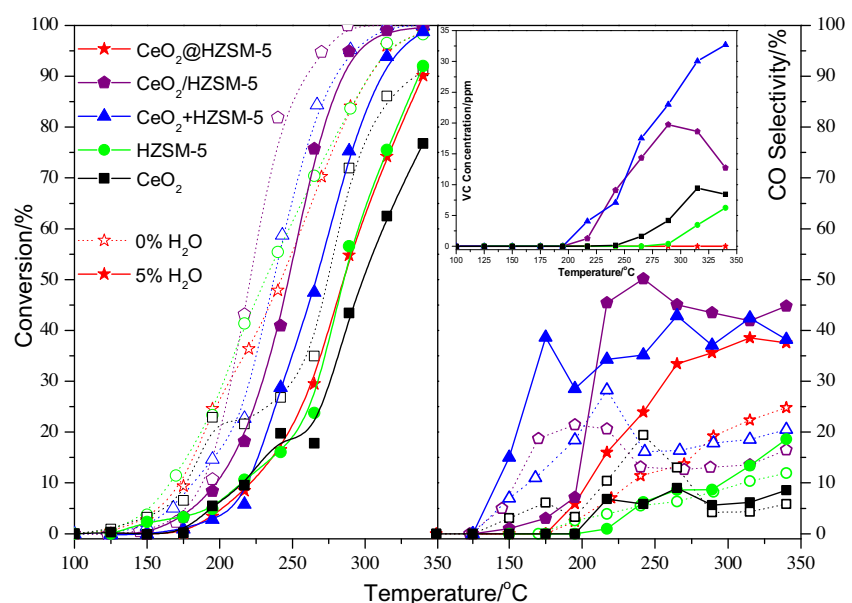


Fig. 12. The effect of water (5 vol.% H₂O) on CeO₂-HZSM-5 composite catalysts and the corresponding concentration of vinyl chloride (VC) and CO selectivity.

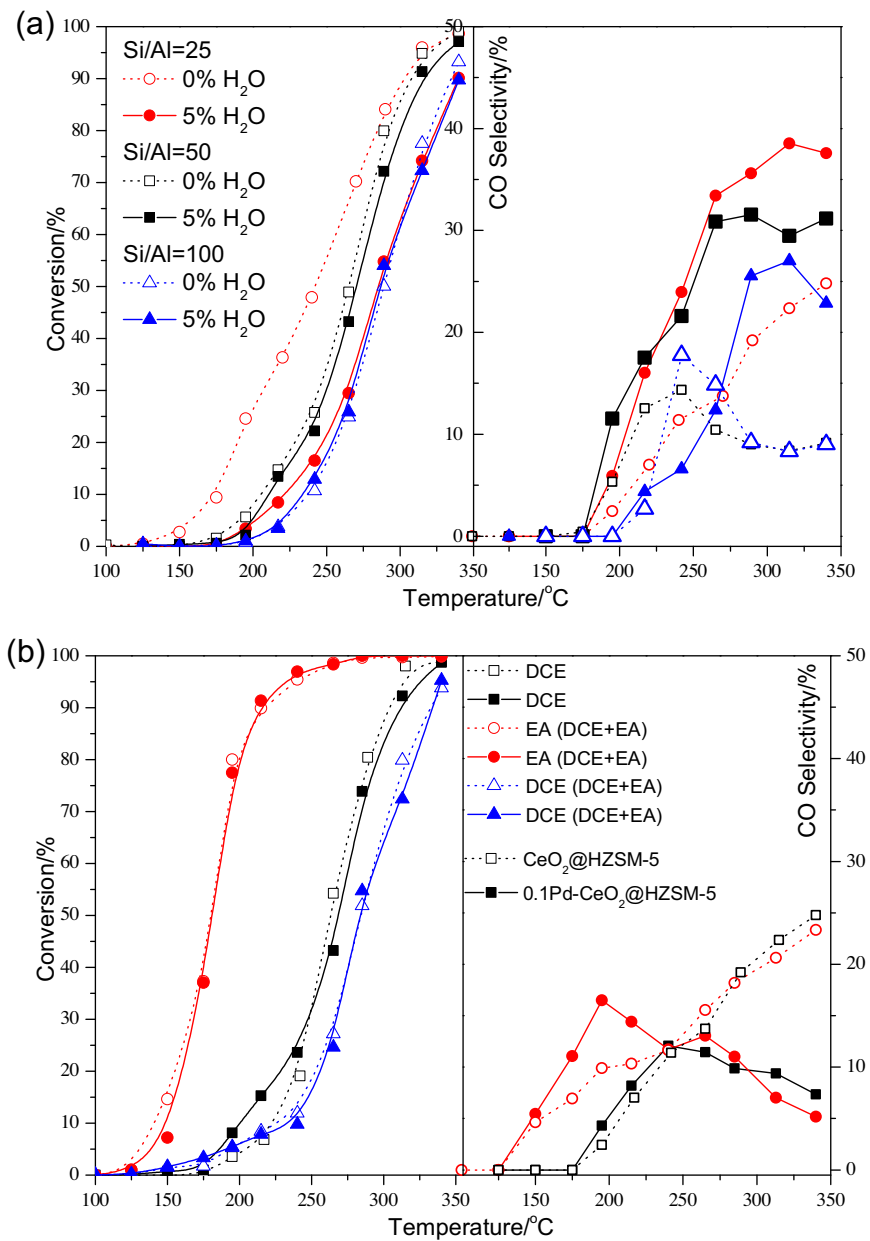


Fig. 13. The effect of water (5 vol.% H₂O) on CeO₂@HZSM-5 with Si/Al ratio (a) and effect of ethyl acetate (EA) on activity and CO selectivity of 0.1Pd-CeO₂@HZSM-5 (b) (1000 ppm DCE and 500 ppm EA, 30,000 m³/h gcat).

tests under humid condition. The inhibition of VC formation was attributed to the competitive adsorption or blocking of H₂O on base sites of CeO₂ and Brønsted acidity sites of HZSM-5 [25]. The formation of active chlorine (Cl₂) was suppressed while the formation of HCl was predominant in the presence of H₂O, which caused the poly-chlorinated by-products not to form *via* the subsequent chlorination pathways (Scheme 1). Surely, the decrease of VC was another factor.

Widely accepted, the hydrophobicity of ZSM-5 zeolite can be adjusted by the control of Si/Al ratio and increases with the increase of Si content. Thus, CeO₂@HZSM-5 catalysts with different Si/Al ratio (the Si/Al ratio of 25, 50 and 100) was prepared to investigate the effects of the hydrophobicity on the oxidation of DCE, and the curves of DCE conversion and CO selectivity vs temperature were displayed in Fig. 13a under dry and humid conditions, to be sure, the real Si/Al ratio was 75, 160 and 300 (determined by XRF), respectively. CeO₂@HZSM-5 with the higher Si/Al ratio showed a

lower catalytic activity for DCE oxidation due to the decrease of surface acid amount, conversely, the inhibition effect of H₂O significantly reduced and disappeared completely when the Si/Al ratio increased to 100. Indeed, it can be found that CeO₂@HZSM-5 catalysts with the Si/Al ratio of 25 and 100 presented a same activity curve in the presence of 5 vol.% H₂O, by comprehensive comparison, CeO₂@HZSM-5 (Si/Al = 100) with appropriate surface acid and hydrophobicity showed an optimum catalytic performance. Additionally, CO selectivity also decreased with the increase of Si/Al ratio. Moreover, the non-chlorinated VOCs, for example 500 ppm ethyl acetate (EA), were added to DCE to evaluate thoroughly the catalytic performance of CeO₂@HZSM-5 as a promising practical catalyst of DCE oxidation (Fig. 13b). EA slightly suppressed the oxidation of DCE and the T₅₀ increased from 260 to 280 °C, while 90% conversion of EA had been obtained at 215 °C. CO selectivity mildly increased in the low temperature ranges (below 250 °C) for the coexisting of DCE and EA, which was attributed to the incomplete

oxidation of EA due to the slow migration of active oxygen species presenting on CeO_2 encapsulated by ZSM-5 at lower temperature, and then slowly increased with the increase of temperature up to 25% (same with single DCE). Meanwhile, 0.1Pd- CeO_2 @HZSM-5 catalyst also was investigated to further depress the CO selectivity, because the strong metal-support interaction (SMSI) between noble metals and CeO_2 was considered generally to can improve the oxygen mobility and reactivity. Compared with CeO_2 @HZSM-5 catalyst, the change of conversion curves of both DCE and EA was almost imperceptible, which was because PdO was completely coated by HZSM-5 and not directly exposed to DCE or EA. However, CO selectivity showed a steady decline in the higher temperature ranges (above 200–225 °C) and reduced to only 5% at 350 °C. Thus, the loading of trace Pd promoted the oxygen mobility of CeO_2 and enhanced its oxidation ability, and more carbon species were easily oxidized into CO_2 . Small amounts of CO were still unavoidable, but there was still room for improvement, for examples, increasing the loading amount of Pd and screening the better noble metals or transition metals to enhance the oxidation ability, or synthesizing the CeO_2 nanosheet encapsulated by ZSM-5 nanosheet or nanosized ZSM-5 particle hybrid composites to promote the diffusion/migration of active oxygen.

4. Conclusions

Considering the coking and chlorine poisoning deactivation of pure HZSM-5 and CeO_2 for catalytic combustion of CVOCs, a novel CeO_2 -HZSM-5 composite material was designed, that is CeO_2 nanosheets encapsulated by HZSM-5 (sandwich core-shell structured CeO_2 @HZSM-5), and investigated in the catalytic total oxidation of DCE as a model reaction. As a reference, CeO_2 /HZSM-5 and $\text{CeO}_2 + \text{HZSM-5}$ were prepared by incipient-wetness impregnation method and physically mixing method, respectively. A series of characterizations such as SEM, H_2 -TPR, NH_3 -TPD were adopted to identify structure and properties of these synthesized materials, the results indicated that CeO_2 @HZSM-5 displayed a sandwich type core-shell structure and CeO_2 nanosheets were completely encapsulated by HZSM-5 particles which formed continuous and dense membranes (exposed HZSM-5), whereas CeO_2 /HZSM-5 and $\text{CeO}_2 + \text{HZSM-5}$ presented a structure exposed CeO_2 (HZSM-5 was coated by CeO_2) and both exposed CeO_2 and HZSM-5 (CeO_2 dispersed on/among HZSM-5 particles), respectively. The first two of these revealed the strong interaction between CeO_2 and HZSM-5, while only physical interaction was observed for $\text{CeO}_2 + \text{HZSM-5}$ (H_2 -TPR results), moreover, no significant difference of acid properties (including acid strength and total acid amount) among these three catalysts was observed. Catalytic oxidation of DCE showed that the catalytic activities were as follows: CeO_2 /HZSM-5 > $\text{CeO}_2 + \text{HZSM-5}$ > CeO_2 @HZSM-5, which was related to the high activity of CeO_2 for CVOCs oxidation and the synergistic effect between CeO_2 and HZSM-5. Expectedly, CeO_2 @HZSM-5 presented the worst activity for the oxidation of DCE (similar with pure HZSM-5), because CeO_2 was completely encapsulated by HZSM-5 and could not be exposed directly to DCE molecules, while the oxidation of DCE occurred via an acid catalytic pathway. Compared with pure CeO_2 and HZSM-5 catalysts, all CeO_2 -HZSM-5 composite catalysts exhibited a better resistance to the coking and chlorine poisoning, however, numerous chlorinated by-products were formed over CeO_2 /HZSM-5 and $\text{CeO}_2 + \text{HZSM-5}$ catalysts, which was attributed to the high activity of the exposed CeO_2 to the cleavage of C-Cl bonds and Deacon reaction. For CeO_2 @HZSM-5 catalyst, the main by-product was only VC, which was formed via the abstraction of HCl on acidity sites of the exposed HZSM-5. The formation of less chlorinated byproducts, especially poly-chlorinated by-products, was equally

important for the catalytic oxidation of CVOCs compared with high activity and good stability, therefore, CeO_2 @HZSM-5 catalyst was more potential for the practical application. Additionally, in the lower temperature ranges (such as 250 °C), the formation of coke on CeO_2 @HZSM-5 catalyst was inevitable, but an excellent stability with a slight oscillation could still be achieved. Coke analysis (TPO, Raman and XPS) showed the coke deposited on CeO_2 @HZSM-5 was mainly comprised of white coke (paraffinic and cyclopentadienyl species) and easier to be removed via *in situ* oxidation by the oxygen species from CeO_2 compared with pure HZSM-5, which was responsible for the superior resistance to the coking deactivation. The H_2O and non-chlorinated VOCs (such as EA) obviously inhibited the oxidation of DCE over CeO_2 -HZSM-5 catalysts mainly due to the competitive adsorption for active sites. However, poly-chlorinated by-products almost completely disappeared owing to the formation of more HCl and less Cl_2 in the presence of H_2O , especially for the catalysts with the exposed CeO_2 . Additionally, the inhibition effect of H_2O declined with the increase of hydrophobicity of HZSM-5 (by the increase of Si/Al ratio), and trace of Pd could significantly promoted the oxidation of CO into CO_2 .

Acknowledgments

This work was supported by the National Natural Science Foundation of China (Nos. 21307033 and 21477036), the Shanghai Natural Science Foundation (No. 13ZR1411000) and the National Key Research and Development Program of China (No. 2016YFC0204300).

Appendix A. Supplementary data

Supplementary data associated with this article can be found, in the online version, at <http://dx.doi.org/10.1016/j.apcatb.2016.10.009>.

References

- [1] A. Aranzabal, B. Pereda Ayo, M.P. González Marcos, J.A. González Marcos, R. López Fonseca, J.R. González Velasco, State of the art in the catalytic oxidation of volatile organic compounds, *Chem. Papers* 68 (2014) 1169–1186.
- [2] J.R. González-Velasco, R. López-Fonseca, A. Aranzabal, J.I. Gutiérrez-Ortiz, P. Steltenpohl, Evaluation of H-type zeolites in the destructive oxidation of chlorinated volatile organic compounds, *Appl. Catal. B* 24 (2000) 233–242.
- [3] R. López-Fonseca, A. Aranzabal, J.I. Gutiérrez-Ortiz, J.I. Álvarez-Uriarte, J.R. González-Velasco, Comparative study of the oxidative decomposition of trichloroethylene over H-type zeolites under dry and humid conditions, *Appl. Catal. B* 30 (2001) 303–313.
- [4] R. López-Fonseca, A. Aranzabal, P. Steltenpohl, J.I. Gutiérrez-Ortiz, J.R. González-Velasco, Performance of zeolites and product selectivity in the gas-phase oxidation of 1, 2-dichloroethane, *Catal. Today* 62 (2000) 367–377.
- [5] R. López-Fonseca, B. de Rivas, J.I. Gutiérrez-Ortiz, A. Aranzabal, J.R. González-Velasco, Enhanced activity of zeolites by chemical dealumination for chlorinated VOC abatement, *Appl. Catal. B* 41 (2003) 31–42.
- [6] M. Gallastegi-Villa, A. Aranzabal, M. Romero-Sáez, J.A. González-Marcos, J.R. González-Velasco, Catalytic activity of regenerated catalyst after the oxidation of 1, 2-dichloroethane and trichloroethylene, *Chem. Eng. J.* 241 (2014) 200–206.
- [7] A. Aranzabal, M. Romero-Sáez, U. Elizundia, J.R. González-Velasco, J.A. González-Marcos, Deactivation of H-zeolites during catalytic oxidation of trichloroethylene, *J. Catal.* 296 (2012) 165–174.
- [8] A. Aranzabal, J.A. González-Marcos, M. Romero-Sáez, J.R. González-Velasco, M. Guillemot, P. Magnoux, Stability of protonic zeolites in the catalytic oxidation of chlorinated VOCs (1, 2-dichloroethane), *Appl. Catal. B* 88 (2009) 533–541.
- [9] R. Rachapudi, P.S. Chintawar, H.L. Greene, Aging and structure/activity characteristics of Cr-ZSM-5 catalysts during exposure to chlorinated VOCs, *J. Catal.* 185 (1999) 58–72.
- [10] B. Ramachandran, H.L. Greene, S. Chatterjee, Decomposition characteristics and reaction mechanisms of methylene chloride and carbon tetrachloride using metal-loaded zeolite catalysts, *Appl. Catal. B* 8 (1996) 157–182.
- [11] J.I. Gutiérrez-Ortiz, R. López-Fonseca, U. Aurrekoetxea, J.R. González-Velasco, Low-temperature deep oxidation of dichloromethane and trichloroethylene by H-ZSM-5-supported manganese oxide catalysts, *J. Catal.* 218 (2003) 148–154.

[12] Q.G. Dai, X.Y. Wang, G.Z. Lu, Low-temperature catalytic destruction of chlorinated VOCs over cerium oxide, *Catal. Commun.* 8 (2007) 1645–1649.

[13] B. de Rivas, C. Sampedro, R. López-Fonseca, M.A. Gutiérrez-Ortiz, J.I. Gutiérrez-Ortiz, Low-temperature combustion of chlorinated hydrocarbons over CeO₂/H-ZSM5 catalysts, *Appl. Catal. A* 417–418 (2012) 93–101.

[14] B. de Rivas, C. Sampedro, E.V. Ramos-Fernández, R. López-Fonseca, J. Gascon, M. Makkee, J.I. Gutiérrez-Ortiz, Influence of the synthesis route on the catalytic oxidation of 1, 2-dichloroethane over CeO₂/H-ZSM5 catalysts, *Appl. Catal. A* 456 (2013) 96–104.

[15] Q.Q. Huang, X.M. Xue, R.X. Zhou, Decomposition of 1,2-dichloroethane over CeO₂ modified USY zeolite catalysts: effect of acidity and redox property on the catalytic behavior, *J. Hazard. Mater.* 183 (2010) 694–700.

[16] J.M. Zhou, L. Zhao, Q.Q. Huang, R.X. Zhou, X.K. Li, Catalytic activity of Y zeolite supported CeO₂ catalysts for deep oxidation of 1, 2-dichloroethane (DCE), *Catal. Lett.* 127 (2009) 277–284.

[17] Q.Q. Huang, X.M. Xue, R.X. Zhou, Influence of interaction between CeO₂ and USY on the catalytic performance of CeO₂-USY catalysts for deep oxidation of 1,2-dichloroethane, *J. Mol. Catal. A* 331 (2010) 130–136.

[18] Q.Q. Huang, X.M. Xue, R.X. Zhou, Catalytic behavior and durability of CeO₂ or/and CuO modified USY zeolite catalysts for decomposition of chlorinated volatile organic compounds, *J. Mol. Catal. A* 344 (2011) 74–82.

[19] P. Yang, X.M. Xue, Z.H. Meng, R.X. Zhou, Enhanced catalytic activity and stability of Ce doping on Cr supported HZSM-5 catalysts for deep oxidation of chlorinated volatile organic compounds, *Chem. Eng. J.* 234 (2013) 203–210.

[20] Q.G. Dai, X.Y. Wang, G.Z. Lu, v Low-temperature catalytic combustion of trichloroethylene over cerium oxide and catalyst deactivation, *Appl. Catal. B* 81 (2008) 192–202.

[21] A.P. Amrute, C. Mondelli, M. Moser, G. Novell-Leruth, N. López, D. Rosenthal, R. Farra, M.E. Schuster, D. Teschner, T. Schmidt, J. Pérez-Ramírez, Performance structure, and mechanism of CeO₂ in HCl oxidation to Cl₂, *J. Catal.* 286 (2012) 287–297.

[22] R. Farra, F. Girgsdies, W. Frandsen, M. Hashagen, R. Schlägl, D. Teschner, Synthesis and catalytic performance of CeOCl in deacon reaction, *Catal. Lett.* 143 (2013) 1012–1017.

[23] Q.G. Dai, S.X. Bai, Y. Lou, X.Y. Wang, Y. Guo, G.Z. Lu, Sandwich-like PdO/CeO₂ nanosheet@HZSM-5 membrane hybrid composite for methane combustion: self-redispersion, sintering-resistance and oxygen, water-tolerance, *Nanoscale* 8 (2016) 9621–9628.

[24] Q.G. Dai, S.X. Bai, H. Li, W. Liu, X.Y. Wang, G.Z. Lu, Template-free and non-hydrothermal synthesis of CeO₂ nanosheets via a facile aqueous-phase precipitation route with catalytic oxidation properties, *CrystEngComm* 16 (2014) 9817–9827.

[25] Q.G. Dai, S.X. Bai, Hua Li, W. Liu, X.Y. Wang, G.Z. Lu, Catalytic total oxidation of 1, 2-dichloroethane over highly dispersed vanadia supported on CeO₂ nanobelts, *Appl. Catal. B* 168 (2015) 141–155.

[26] Q.G. Dai, S.X. Bai, X.Y. Wang, G.Z. Lu, Facile synthesis of HZSM-5 with controlled crystal morphology and size as efficient catalysts for chlorinated hydrocarbons oxidation and xylene isomerization, *J. Porous Mater.* 21 (2014) 1041–1049.

[27] J.C. Groen, J. Perez-Ramirez, Critical appraisal of mesopore characterization by adsorption analysis, *Appl. Catal. A* 268 (2004) 121–125.

[28] G. Sinquin, C. Petit, S. Libs, J.P. Hindermann, A. Kiennemann, Catalytic destruction of chlorinated C2 compounds on a LaMnO₃₊₍₊₎ perovskite catalyst, *Appl. Catal. B* 32 (2001) 37–47.

[29] Q.G. Dai, S.X. Bai, J.W. Wang, M. Li, X.Y. Wang, G.Z. Lu, The effect of TiO₂ doping on catalytic performances of Ru/CeO₂ catalysts during catalytic combustion of chlorobenzene, *Appl. Catal. B* 142 (2013) 222–233.

[30] Y.T. Chua, P.C. Stair, An ultraviolet Raman spectroscopic study of coke formation in methanol to hydrocarbons conversion over zeolite H-MFI, *J. Catal.* 213 (2003) 39–46.

[31] C.P. Li, Y.W. Chen, S.J. Yang, R.B. Yen, In-situ FTIR investigation of coke formation on USY zeolite, *Appl. Surf. Sci.* 8 (1994) 465–468.

[32] X.C. Li, S.G. Li, Y.F. Yang, M. Wu, F. He, Studies on coke formation and coke species of nickel-based catalysts in CO₂ reforming of CH₄, *Catal. Lett.* 118 (2007) 59–63.

[33] B.de Rivas, R. López-Fonseca, M.A. Gutiérrez-Ortiz, J.I. Gutiérrez-Ortiz, Role of water and other H-rich additives in the catalytic combustion of 1, 2-dichloroethane and trichloroethylene, *Chemosphere* 75 (2009) 1356–1362.

[34] F. Bertinchamps, A. Attianese, M.M. Mestdagh, E.M. Gaigneaux, Catalysts for chlorinated VOCs abatement: multiple effects of water on the activity of VO_x based catalysts for the combustion of chlorobenzene, *Catal. Today* 112 (2006) 165–168.

[35] Q.G. Dai, L.L. Yin, S. Bai, W. Wang, X.Y. Wang, X.Q. Gong, G.Z. Lu, Catalytic total oxidation of 1, 2-dichloroethane over VO_x/CeO₂ catalysts: further insights via isotopic tracer techniques, *Appl. Catal. B* 182 (2016) 598–610.